STRUCTURAL QUALIFICATION OF THE ORBITING ASTRONOMICAL OBSERVATORY

W. Brian Keegan
NASA, Goddard Space Flight Center
Greenbelt, Maryland

After the failure of Orbiting Astronomical Observatory I (OAO-I) shortly after launch, a recovery effort was mounted in all disciplines associated with the program. In the structures area, this consisted of a review of basic spacecraft design concepts with subsequent development of an overall structural qualification test plan. This plan outlined both a series of environmental tests and the supporting dynamic analyses required to verify the integrity of the OAO structure. A summary of this structural qualification effort is presented in this paper.

The introductory portion of the paper traces briefly the evolution of the structural test criteria from the point of preliminary analysis to the definition of meaningful test requirements. The paper then concerns itself with the implementation of these structural test requirements. Although static load testing was considered, it was decided that qualification of the OAO structure could best be accomplished using the Launch Phase Simulator (LPS) at the Goddard Space Flight Center.

Three loading conditions were required for this qualification test: one using the LPS centrifuge and the other two using the LPS vibration system, one of these employing simultaneous longitudinal and lateral vibration inputs. The paper places major emphasis on this multi-axis vibration test, discussing the reasons for conducting it, the methods of controlling the phase and frequency relationships of the two inputs, and the accuracy to which the desired loads were obtained.

The paper then presents a discussion of combined environment testing performed on the LPS to qualify such secondary structural items as thermal skins, sun baffles and solar arrays. It concludes with an outline of the four-environment (acceleration, vibration, acoustics and vacuum) test envisioned for future OAO flight observatories on the LPS.

INTRODUCTION

The Orbiting Astronomical Observatory, hereafter referred to simply as OAO, is a precisely stabilized orbiting optical telescope whose purpose is to provide astronomical measurements from above the obscuring influences of the earth's atmosphere, principally in the far ultraviolet region of the electromagnetic spectrum.

Depicted in Figure 1 in the orbital configuration, the observatory is 14 feet long and 20 feet wide with the solar arrays, inertial booms and sunshade extended. The main body is a 10-foot long, 80-inch wide octagon with a 4-foot diameter center tube running its entire length for housing of the optical elements of the primary experiments.

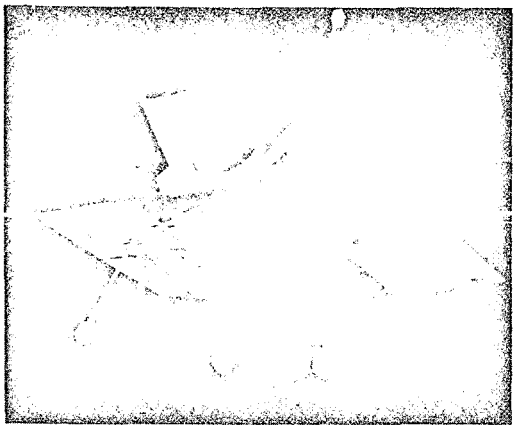

Figure 1. Artist's Concept of Orbiting Astronomical Observatory in Orbital Configuration

The guidance, control, data handling equipment and the like are in turn mounted in the 48 bays surrounding the center tube. Total observatory weight is approximately 4400 pounds, 1000 pounds of which is allocated for experiments.

OAO-II, successfully launched in December of 1968 into a 400 nautical mile circular orbit by an Atlas/Centaur launch vehicle, contained two optical experiments, each viewing from opposite ends of the center tube. The University of Wisconsin Experiment Package is currently providing data on the energy distribution of various stars and star clusters in the far-ultraviolet light field. Meanwhile, the Smithsonian Astrophysical Observatory's Celescope Experiment is measuring the brightness of approximately 50,000 main-sequence stars in this same far-ultraviolet light field.

OAO-I, meanwhile, launched in April of 1966, had failed before returning any useful data from its experiments. As a result, a recovery effort was mounted in all disciplines associated with the program in order to assure the success of all future OAO missions. In the structures area, this consisted of a thorough review of the observatory design concepts with the subsequent development of an overall structural qualification test plan which outlined both a series of environmental tests and the supporting analyses required to verify the structural integrity of the observatory.

EVOLUTION OF TEST CRITERIA

One of the prime analytic requirements of this overall structural qualification plan was a flight dynamic loads analysis, which was performed by the launch vehicle contractor. Goddard's contribution to this loads analysis was a lumped-mass model of the OAO observatory with the optical experiments represented as a single-mass branch off the nine-mass main beam representation of the observatory primary structure. For Goddard's in-house purposes, however, a far more sophisticated finite-element model of the observatory was developed containing 128 grid points and 588 degrees of freedom. For structural dynamics purposes, it was used to compute the modal loads and displacements for the first 20 resonant frequencies. Additionally, it was used to evaluate thermally induced optical misalignments.

The necessary interrelationship between analytic investigation and experimental investigation was pointed up vividly during the OAO-II program. The first cantilevered lateral bending mode of the OAO observatory is highly

affected by the stiffness of the interstage adapter and particularly by the compliance of the launch vehicle/observatory interface joint. For obvious reasons, the compliance of this joint could not be confidently modelled, and it fell to the modal survey vibration test to supply this needed information. The actual method employed in extracting this information was to adjust the compliance of the interface joint until the computed frequency of the first lateral bending mode agreed with the frequency determined for that mode during the modal survey vibration test. After this adjustment was made to the model, excellent correlation was obtained between the analytic and experimental results for all of the significant modes.

The flight dynamic loads analysis showed that there were three flight conditions responsible for introducing the critical loads into the OAO structure. These occurred at:

1. Lift-off - when the maximum lateral bending loads, induced by a highly directional transient introduced by the launcher release mechanism, were coupled with a combined steady-state and oscillatory longitudinal load,

2. Atlas Booster Engine Cut-off - when the maximum compressive loads were induced by maximum vehicle steady-state acceleration, and

3. Centaur Main Engine Cut-off - when the maximum tensile loads were induced by the "elastic rebound" effects caused by thrust termination.

The final report on the flight dynamics loads analysis expressly stated that the results of any high frequency environmental effects were not included in the analysis, but that appropriate factors should be added to the results. It was felt at Goddard that the environmental effects at Atlas Booster Engine Cut-off and at Centaur Main Engine Cut-off would be negligible since these conditions occurred out of the atmosphere. At Lift-off, however, they were the most severe of the entire flight regime and some additive factor for their load contribution had to be made. The following rationale resulted, therefore, in defining this factor for estimating the Lift-off environmental effects:

1. The Goddard general environmental test specification defines a random vibration test spectrum which essentially accounts for these high-frequency environmental effects. This spectrum is derived from flight data and should induce loads during the random vibration test representative of those expected during launch due to these environmental effects.

2. Strain gage data was available which correlated strains induced in critical OAO structural members with this same random vibration spectrum shape.

3. Strain gage data was also available which correlated the strains induced in the same structural members to a given bending load at the base of the spacecraft. This spacecraft interface load had been computed by using the accelerations actually measured at various OAO stations during a sinusoidal vibration test in conjunction with the lumped mass weight breakdown of the observatory used in the flight loads analysis.

4. By comparing these strain data from the sinusoidal and random vibration tests, an equivalent maximum bending load induced by the random vibration test and hence by the environmental effects was obtained. An rms summation of this load with the predicted launch release transient load was then made to form the maximum flight bending load.

5. A similar process was used to evaluate the longitudinal loads induced in the structure at Lift-off by these environmental effects.

Three loading conditions were necessary, therefore, to obtain qualification of the OAO structural design. Table I presents the loads corresponding to each of these conditions. It will be noted that the design qualification loads are 1.5 times the flight loads in accordance with the Goddard philosophy of demonstrating a design margin of 50 percent in excess of flight loads.

It should be noted that the effects of the torsional transients induced by the Atlas/Centaur launch vehicle were evaluated and considered to be of no consequence. Therefore, torsional vibration testing was eliminated from consideration.

SELECTION OF TEST FACILITY

Although not mentioned in the previous section, it was desired to impose both the lateral and longitudinal loads during the simulation of the Lift-off loading condition. While these longitudinal loads were not critical, they were substantial since they occurred in combination with the maximum lateral loads. Consideration was therefore given first to conducting a static load test, and although excellent simulation could have been achieved by this method, the schedule and cost viewpoints forced a search for a different approach.

An investigation of the load distributions required showed that excellent correlation was attainable between the "in-flight" and "on the shaker" load distributions for the Centaur Cut-off (maximum tension) and Lift-off (maximum bending) conditions. This is illustrated for the tension case in Figure 2 where the OAO acceleration and load distributions predicted at Centaur Cut-off are compared with those obtained on the shaker at the first longitudinal resonance. This favorable comparison is attributed to the fact that the node of the Centaur/OAO first longitudinal mode lies near the Centaur/OAO interface plane, thus giving the OAO portion of this mode shape the appearance of a first cantilevered mode. Similarly, favorable comparisons for the bending case are presented in Figure 3. These are attributed to the fact that the first lateral cantilevered mode shape of the OAO shows no elastic deformation of the primary structure, but rather

TABLE I

OAO STRUCTURAL QUALIFICATION LOADS

Flight Condition	Type Load	Flight Load			Qual. Load
		Dynamic	Environmental	RMS Sum	
Lift-off	Bending	527,000 in-lb	141,000 in-lb	546,000 in-lb	821,000 in-lb
Atlas Cut-off	Compression	29,590 lb	0	29,590 lb	44,385 lb
Centaur Cut-off	Tension	8,700 lb	0	8,700 lb	13,050 lb

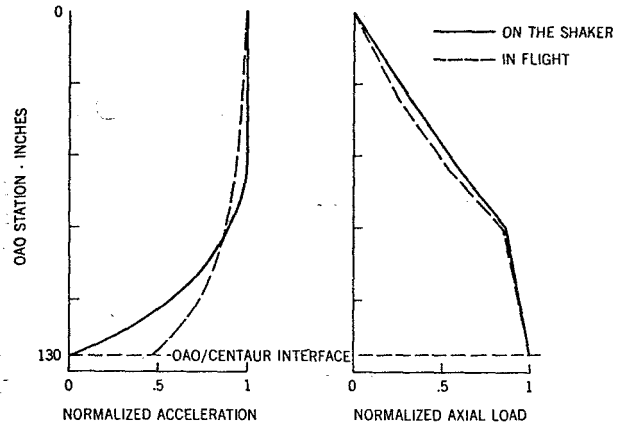

Figure 2. OAO Longitudinal Response - In Flight vs. On The Shaker

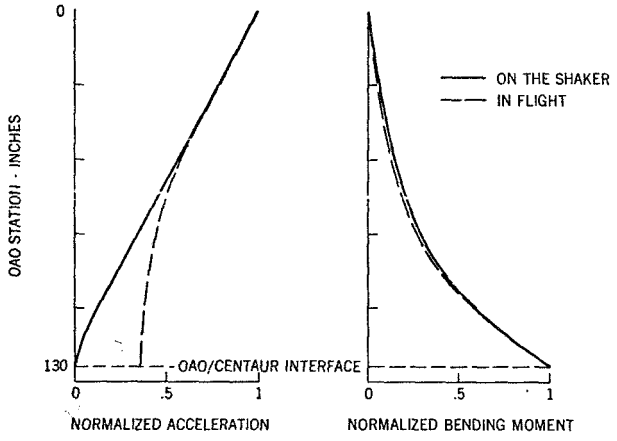

Figure 3. OAO Lateral Response - In Flight vs. On The Shaker

rotation of the entire observatory about the highly compliant interface joint discussed previously. Therefore, the observatory's "on the launch vehicle" behavior resembled its "on the shaker" behavior.

Since the Goddard Launch Phase Simulator (LPS) had multi-axis vibration capability, thereby permitting the desired simulation of the Lift-off condition, it was decided to perform the maximum tension and maximum bending loading conditions using the LPS off-board vibration system and the maximum compression loading condition using the LPS centrifuge.

Since the Launch Phase Simulator is such a unique facility, a brief description of its capabilities will be presented here. For those interested, more detailed information is contained in References (1) and (2).

The centrifuge, depicted in an overall view in Figure 4, has a nominal radius of 60 feet, and is capable of accelerating a test article to 30G. Capability exists in the arm drive system for matching the real-time acceleration onset rate for all but sounding rocket class launch vehicles. The test item itself is enclosed in the test chamber during the test, mounted to the end-cap with its thrust axis oriented horizontally. The test item is mated to the end-cap while in the vertical position. The specially designed six-degree-of-freedom LPS handling vehicle then picks up the end-cap, pitches it from vertical to horizontal and mates the end-cap to the test chamber. The LPS test chamber contains acoustic and vacuum capabilities about which more will be mentioned later in the discussion.

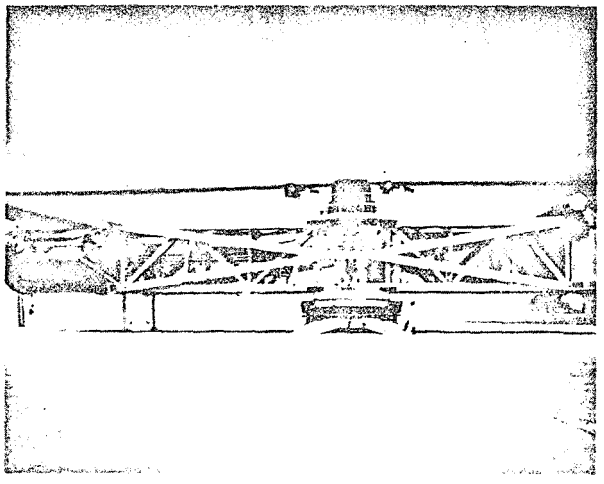

Figure 4. Launch Phase Simulator - Overall View

The LPS vibration system is housed in the end cap. It can be operated either on the arm or in the off-board mode while the end cap is

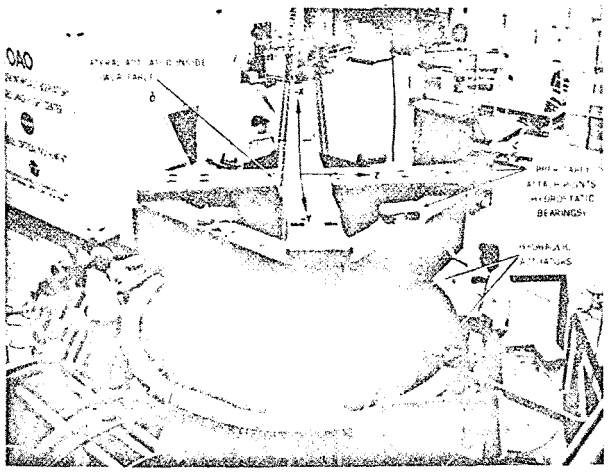

Figure 5. LPS Vibration System View of End-Cap and Lower Vibration Table During Assembly

bolted to a seismic mass located in the LPS preparation area. Figure 5 shows the partially assembled vibration system in this off-board area. The system is composed principally of five hydraulic actuators and two vibration tables all mounted within the end-cap. Three degrees of freedom of vibration are attainable. Two of these are generated by the four thrusting actuators located 90 degrees apart in the base of the end cap (two of these are visible in Figure 5). Operating all four in phase creates a thrusting mode and 48,000 force pounds are available for this operation. A yaw mode, rotation in the X-Z plane about the Y axis, is obtained by operating the two actuators shown in Figure 5 out of phase. This vibration mode was not used during the OAO design qualification test. Figure 5 also shows the lower table being mounted to these actuators. The magnesium table forms the basic support for the entire system. It also contains the fifth actuator, which provides lateral vibration along the Z axis. Figure 6 shows the upper vibration table, which is driven by the lateral actuator. This upper table is an aluminum honeycomb sandwich plate with a series of ring and radial stiffeners. It mates to the lower table by a series of eight hydrostatic bearings which provide

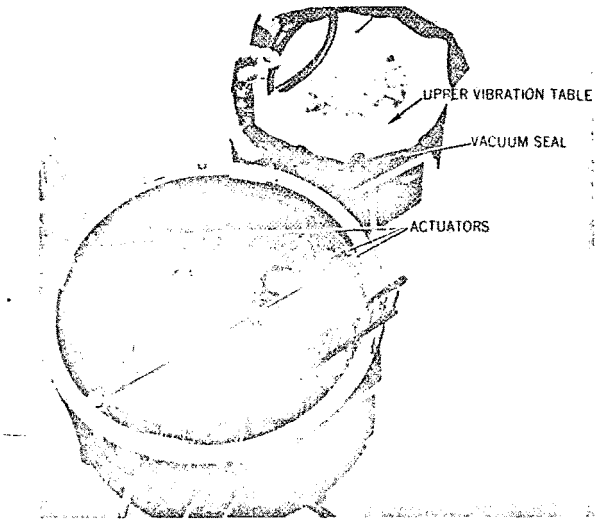

Figure 6. LPS Vibration System - View of End Cap with Lower Vibration Table Removed

support for this table to follow the thrust and yaw vibration inputs while allowing it freedom to follow the lateral input. The test item then mounts to the upper vibration table.

The vacuum seal denoted in Figure 6 serves as a contamination seal keeping the free hydraulic fluid which escapes from the actuator and bearings away from the test item. It simultaneously allows overpressurization of the end cap cavity in order to equalize the centrifugal loads imposed on the vibration tables so that these loads will not have to be supported by the thrusting hydraulic actuators.

STRUCTURAL QUALIFICATION TEST SEQUENCE

Exact simulation of the lateral portion of the Lift-off condition was possible once it was determined that the "on the shaker" load distribution matched that predicted for flight. The same was not true, however, for the longitudinal portion. Table II summarizes the longitudinal loads at Lift-off and it can be seen that the predicted flight load was 1.20G compression due to launch vehicle thrusting, plus and minus the

TABLE II

OAO LONGITUDINAL LOADS AT LIFT-OFF

Predicted for Flight:

Static	+1.20 G
Dynamic	±0.58 G
Environmental	±0.56 G
Total	+1.20 ±0.80 G

Qualification Load:

Total	+1.80 ±1.20 G

Desired Load Envelope:

+1.8 ±1.2 G
(+3.00 to +0.60)

Attainable Load Envelope:

+1.0 ±2.0 G
(+3.00 to -1.00)

oscillatory load of .80 G, where the .80 is derived from the rms summation of the dynamic and environmental contributions. Applying the safety factor of 1.5 gives the qualification loads shown, and in turn yields the longitudinal load envelope oscillating between a maximum of +3.0 G and a minimum of +0.6 G. On the shaker, of course, any oscillation occurs about a mean of +1.0 G (the compression load due to gravity). Thus, in order to match the maximum side of the required envelope at +3.0 G, we necessarily had to accept a minimum loading of -1.0 G as is shown in the Attainable Load Envelope portion of Table II. This meant that a tension load would be applied to the spacecraft, when in fact, none was predicted for this flight condition. This was, however, considered to be an acceptable overtest principally because the tension load imposed here would be significantly lower than the tension load required by the Centaur Burnout condition. In addition, it will be shown later that because of the relationship between the two waveforms, the overtest was not quite as severe as indicated here.

The predominant response frequencies to this lift-off transient were predicted to be approximately 9 Hz laterally and 6 Hz longitudinally. Since the predicted spacecraft load distribution due to the 9 Hz input correlated well with that distribution developed at the first lateral cantilevered mode on the shaker, it was decided to simulate the lateral portion of the launch transient by shaking laterally at the fundamental resonant frequency, approximately 10 Hz, along the axis which the loads would be imposed in flight.

The predicted longitudinal oscillation indicated a rigid-body spacecraft oscillation and therefore any frequency where the cantilevered spacecraft response was essentially rigid-body would have been acceptable for test purposes. Consideration was given to shaking longitudinally at about 6 Hz, but this was discarded in favor of shaking longitudinally at a frequency somewhat above the lateral input frequency. This decision was made because the displacement required at the higher frequency for the same input acceleration level is substantially less and because the lateral cross-talk induced by the longitudinal input would be greatly reduced by shaking longitudinally at a frequency above the first lateral resonant frequency.

The principal objective, of course, was to simultaneously induce the worst-case loads due to the combination of the dual-axis vibration inputs. To accomplish this, it was necessary to control the phase and frequency relationships between the longitudinal and lateral inputs. By shaking longitudinally at four-thirds the lateral frequency and by properly maintaining the desired phase relationship between the two input signals, it was possible to envelope the maximum and minimum loads on both sides of the spacecraft during the same run. The required phase and frequency relationship between the thrust and lateral input accelerations and the response due to these inputs is illustrated in Figure 7. As can be seen from this figure, maximum loading due to both the longitudinal and the lateral inputs occurs simultaneously in truss A at time T_1

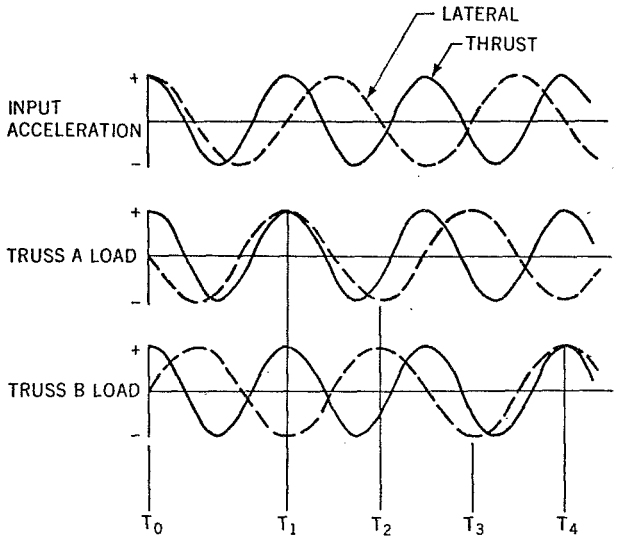

Figure 7. Planned OAO Lift-off Simulation Waveforms - Lateral and Thrust

and in truss B (opposite truss A) at time T_4. Similarly, minimum loading due to the lateral input occurs simultaneously with a zero axial load due to the longitudinal input in truss A at time T_2 and in truss B at time T_3. It will be noted that since the lateral input occurs at the resonant frequency, the load response leads the input by 90 degrees on one side of the structure and lags the input by 90 degrees on the other side. Since the longitudinal input occurs in the region where the spacecraft response is rigid body, however, both the input and response are in phase.

The mechanism used to maintain the desired relationship between the lateral and longitudinal waveforms was a specially designed manually controlled two-axis phase control system. Frequency control was accomplished by means of a frequency division circuit which provided frequency outputs with a four to three ratio between them. Phase control was then obtained by feeding these two outputs through variable bandpass filters, and by varying the bandpass of one of the filters any desired phase relationship could be obtained between the two signals. Separate servo control systems were then used for each signal so that the two vibration amplitudes were independent both of the frequency and phase parameters and of one another.

The test sequence followed for this test condition consisted first of conducting a low-level sweep to locate the first lateral resonance and therefore the lateral input frequency. Next, an evaluation was made of the lateral cross-talk induced by a longitudinal vibration input in the frequency range of interest. After determining that the cross-talk magnitude was acceptable, the required input levels needed to develop the desired loads were calculated using the low-level acceleration responses measured along the length of the observatory structure in conjunction with the lumped-mass mathematical model of the OAO structural model spacecraft.

Prior to conducting any multi-axis runs, the spacecraft was removed from the vibration table and the inputs were adjusted to obtain the desired relationship between the lateral and longitudinal waveforms. After replacement of the spacecraft onto the table, the inputs were retuned using a low-level input in both axes. For all multi-axis runs, the longitudinal input was brought to level first. Then, the lateral input, since it contributed the major portion of the load, was brought to level for five seconds at which time both inputs were terminated. Intermediate test runs were made at flight level loads, 1.25 times flight level loads and at qualification loads. The inputs required for each successive load increment were re-extrapolated after each run to evaluate structural integrity and the nonlinearity of structural response.

The Centaur cut-off condition was also simulated with the LPS vibration system. As mentioned previously, investigation showed that the in-flight load distribution for this condition was closely approximated by the load distribution in the first longitudinal cantilevered mode shape of the spacecraft. By vibrating the

spacecraft longitudinally at its first resonance, it was possible to induce the proper maximum tension load while still not exceeding the peak compression loads required by the Atlas Burnout condition discussed later.

Testing to this load condition involved only longitudinal vibration and consisted initially of a low-level sweep to define the first resonant frequency. Extrapolations were then made, using the previously mentioned lumped-mass model together with the acceleration responses measured along the length of the structure to define the required input for flight level loads, 1.25 times flight loads, and design qualification loads. As with the Lift-off condition, the required inputs for each successive load increment were re-extrapolated using data from each preceding run.

The Atlas Cut-off condition was a straightforward static acceleration test simulated using the LPS centrifuge. The desired compression load at the observatory base was related to G's at the observatory center of gravity which was in turn related to the RPM of the centrifuge, against which the test was controlled. When mounted on the centrifuge, the observatory longitudinal centerline was canted upward so that at the qualification load levels the resultant acceleration vector including gravity would lie along this centerline. The acceleration gradient over the length of the observatory was 19 percent. This introduced at the base of the observatory a zero shear load and a 6100 inch-pound bending moment, which is equivalent to 0.02 G at the observatory center of gravity.

RESULTS OF QUALIFICATION TEST SEQUENCE

Table III summarizes the results of the qualification test from a load standpoint. It can be readily seen that all loads are well within the permissible 10 percent tolerance band. Of more interest to the test engineer, however, is the accuracy to which the multi-axis vibration inputs were controlled. Figure 8 shows the resultant response waveforms for both the longitudinal and lateral sensing accelerometers mounted at the top of the observatory structure, as well as the strain gage response waveforms at the base of trusses A and B. The times T_1, T_2, T_3 and T_4 refer to the times previously defined in Figure 7. It can be seen from Figure 8 that maximum loading occurs in truss A at T_1, when both the lateral and thrust accelerations reach a maximum. Maximum truss B loading occurs at T_4 when the thrust acceleration reaches maximum as the lateral acceleration reaches minimum. It should be noted that by the convention used here a positive lateral acceleration induces a compression load

TABLE III

OAO QUALIFICATION TEST RESULTS

Condition	Load	Desired	Actual	Error
Lift-off	Bending (in-lb)	821,000	748,000	-8.9%
	Compression (lb)	14,280	14,185	+0.7%
	Tension (lb)	0	100	-
Atlas Cut-off	Compression (lb)	44,385	43,002	-3.2%
Centaur Cut-off	Tension (lb)	13,050	13,139	+0.7%

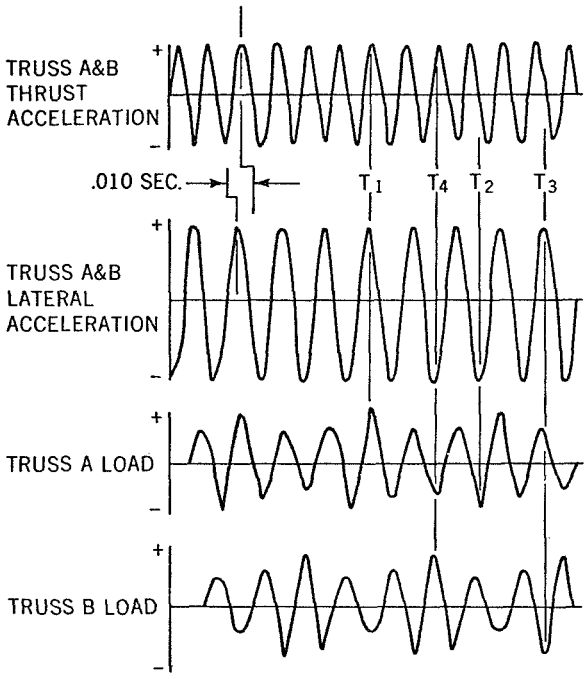

Figure 8. Actual OAO Lift-off Simulation Response Waveforms - Lateral and Thrust

at the base of truss A and a tension load at the base of truss B. A positive thrust acceleration, of course, induces a positive response throughout the structure. Similar appropriate combinations of thrust and lateral accelerations induce minimum loading in truss A at T_2 and in truss B at T_3.

The delay in simultaneous peak occurrences of the two acceleration waveforms of .010 seconds noted in Figure 8 corresponds to a 13 degree lag of the longitudinal waveform with respect to the lateral. As a result, the loading due to the longitudinal input was 97 percent of maximum when the loading due to the lateral input reached maximum. The initial synchronization of the longitudinal and lateral waveforms was established with low-level inputs (about 15 percent of that used for the qualification level input). Undoubtedly, the oscilloscope display of the Lissajous pattern was initially adjusted far more accurately than within 13 degrees. This observed shift is attributed, therefore, to the fact that the resonant frequency shifts slightly as a function of input acceleration. As the vibration levels increase, the phase angle between the lateral input and the lateral response shifts from the optimal 90 degree point, thus introducing the observed error.

This resonant frequency shift is further borne out by the highly nonlinear lateral response encountered during the various incremental runs of the lift-off simulation test. For example, based on the low level sweep data, an input of ±.33 G would have developed the qualification level bending moment. In fact, however, an input of ±.60 G developed a load 8.9 percent less than qualification level.

Much data had been accumulated from previous OAO tests and none exhibited this degree of nonlinearity. During these tests, linear extrapolations had provided extremely accurate predictions of loads developed during specification level runs. These tests had been sweep tests, however, not discrete frequency dwell tests, and it is felt that this dwelling at the same frequency for each run accentuated the effects of the nonlinearity. The resonant frequency shifts slightly as the input amplitude is increased. When sweeping the shaker driving frequency, there always exists a time at which the input frequency coincides with the resonant frequency, and at this time the maximum transmissibility is obtained. When dwelling at one discrete frequency, however, maximum transmissibility will be obtained only if this frequency coincides with the resonant frequency. Therefore, as the resonant frequency moves away from the dwell frequency, the developed transmissibility decreases, thus producing the nonlinear response seen during this test sequence.

ADDITIONAL COMBINED ENVIRONMENT TESTS

In addition to qualification of the primary structure, certain OAO subsystems were subjected to a combined acoustic-venting test using the LPS test chamber as the facility. This type of test is rapidly being accepted by most Goddard programs as a necessary part of their environmental test sequence. The environmental combination of acoustics with pressure venting can impose significant loads on subsystems

which are required to vent the atmospheric pressure. Such a test was run on the OAO solar arrays and the thermal control system which consisted of the previously mentioned sun shades, plus aluminized mylar insulation and alzak foil skins.

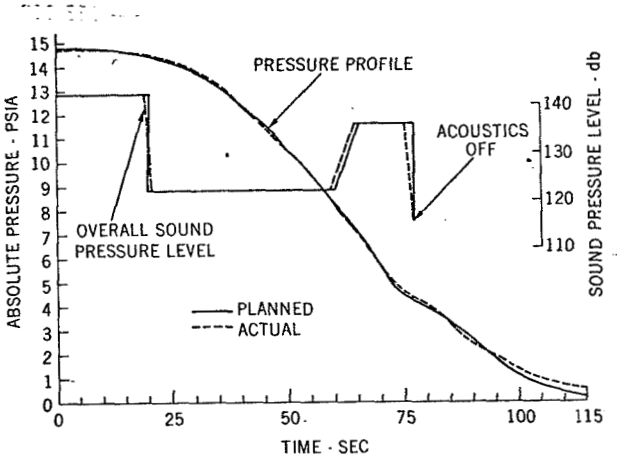

Figure 9. Combined LPS Acoustic-Vacuum Profiles During OAO Thermal Model Tests

The test profile, as shown in Figure 9, consisted of a real-time vacuum pumpdown from ambient through 1 torr, equivalent to an altitude of 150,000 feet, in conjunction with a real-time simulation of the overall acoustic noise level from engine ignition through Mach 1. The steam-ejection type vacuum system of the LPS is capable of matching the real-time pressure profile of all but sounding-rocket class launch vehicles. The acoustic system cuts off automatically as the ambient chamber pressure drops below 50 torr. In flight, however, all significant acoustic excitations terminate well below the 50 torr altitude of 60,000 feet. The acoustic spectrum shape can be equalized prior to conducting a test. This is generally done with some "dummy" test item filling the proper volume of the test chamber. During the actual test run, however, only the overall acoustic level can be varied. The desired and resultant spectra used during the OAO test are shown in Figure 10. The tolerance

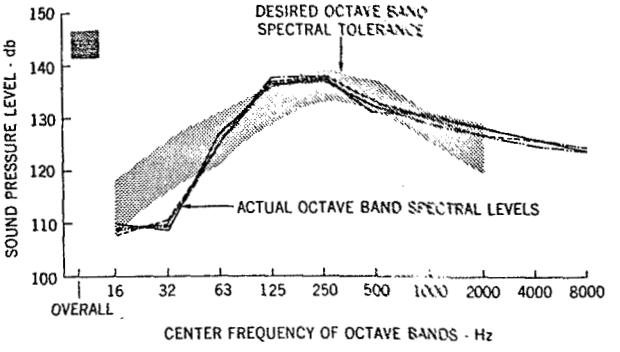

Figure 10. Acoustic Distribution in LPS Test Chamber During OAO Thermal Model Tests

bands on the desired spectra are denoted by the shaded area. The four lines indicate the acoustic spectrum achieved at each of four microphones located at 90 degree intervals around the OAO structural model. As can be seen, the energy distribution around the test chamber was nearly identical and the spectral distribution was outside the specified tolerance limits in only one octave band.

The LPS vibration system, although already used for flight program testing, is presently undergoing modifications to both its table support system and automatic control system [see Reference (3)]. This updated control system contains provisions for automatically controlling the multi-axis phase relationships, thus eliminating the manual operation required during the OAO qualification test. Looking toward the future and the return of the vibration system to operational status, we anticipate performing an "all-up" combined environment test of follow-on OAO observatories.

A plan for such a test was prepared from a review of the flight regime inputs. The various environments were determined to combine most significantly at:

a. Liftoff - when both acoustic noise and the vibration environments (both sinusoidal

and random) are most severe and occur simultaneously with a low steady-state acceleration load,

b. Transonic Region - when both acoustic noise and atmospheric venting are severe and occur in conjunction with a moderate steady-state acceleration load, and

c. Booster Engine Cut-Off - when the quasi steady-state loads due to atmospheric venting are at a potential maximum simultaneously with the maximum steady-state acceleration load.

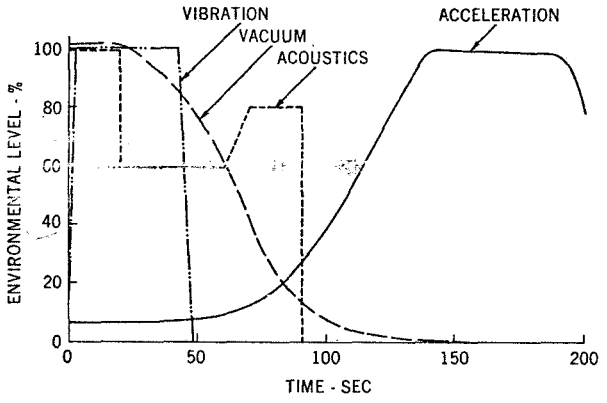

Figure 11. Proposed LPS Combined Four-Environment Test Profile

The proposed environmental profiles are depicted in Figure 11. The vibration portion of the proposed test would consist of two axis (longitudinal and one lateral) sinusoidal and random vibration. The two swept sinusoidal frequencies would be separated from one another by some fixed frequency increment in order to minimize the effects of coupling. Since the LPS imposes an inherent 1G side load when the test item is mounted on the arm, the sine vibration sweep would be limited to frequencies above those which impose critical loads on the test article primary structure. Since most of the vibration encountered during launch occurs at lift-off, the vibration profile will be nearly complete before initiating the real-time simulation of the other three environments. It will be noted, however, that there is a low-level acceleration load imposed during the vibration profile. This is a .3 G load imposed because the LPS arm must be rotating at least at 5 RPM when operating the vibration system in order to avoid uneven wear on the thrust bearing. The lift-off portion of the acoustics profile would be programmed to terminate with the vibration profile, at which time the ancitipated real-time acoustic, venting, and acceleration profiles would be imposed, culminating with a one-minute hold when the maximum acceleration level is reached.

In conclusion, we at Goddard feel that this type of test approach, that is, combined environment testing, is a far better evaluator of spacecraft system performance, simultaneously imposing in a real-time profile most of the significant launch environments. Application of the most critical structural loads would still be reserved, however, for the more controllable single-environment tests, whether they be conducted on a centrifuge, on a vibration exciter, or in a static load test facility.

ACKNOWLEDGMENT

The author particularly wishes to thank Messrs. H. D. Cyphers, J. J. Kerley, E. J. Skolka and W. M. Traylor of the Launch Phase Simulator staff for their invaluable assistance in planning and conducting the qualification test described in this paper.

REFERENCES

(1) Edward J. Kirchman and Charles J. Arcilesi, "Advanced Combined Environmental Test Facility", Shock and Vibration Bulletin No. 37, Part 3, pp. 175-191, January 1968.

(2) Charles J. Arcilesi, "Investigation of Dynamic Characteristics of a 1/20th Scale Model of the Launch Phase Simulator", Shock and Vibration Bulletin No. 35, Part 3, pp. 207-226, January 1966.

(3) Harry D. Cyphers and John F. Sutton, "Control Techniques for Simultaneous Three-Degree-of-Freedom Hydraulic Vibration System", Shock and Vibration Bulletin No. 39, Part 2, pp. 23-33, February 1969.